

$$I(n_N) = C_B I_B(n_N) + C_N I_N(n_N)$$

$$I(n_O) = C_B I_B(n_O) + C_N I_N(n_O)$$

where  $C_B$  and  $C_N$  are the relative populations for the bonded (B) and nonbonded (N) conformers, respectively, and they satisfy  $C_B + C_N = 1$ . One must here note that the relative PIES intensity for the  $n_O$  orbital remains nearly the same for the bonded and nonbonded conformers ( $a_1$  and  $a_3$  in Figure 4,  $a_4$  in Figure 3, and Table II). MO calculations also showed that exterior electron distributions for the  $n_O$  orbitals are rather insensitive to the changes in conformation. Thus one may assume that

$$I_B(n_O) = I_N(n_O)$$

and one obtains

$$I(n_N)/I(n_O) = C_B I_B(n_N)/I_B(n_O) + C_N I_N(n_N)/I_N(n_O)$$

One may then introduce a relationship with the enthalpy and entropy changes due to dissociation of the hydrogen bond

$$\ln K = \ln (C_N/C_B) = -\Delta H/RT + \Delta S/R$$

A least-squares fit to this equation with the observed ratios of  $I(n_N)/I(n_O)$  in Table III leads to the following results:

$$\Delta H = 1.25 \text{ kJ mol}^{-1} \text{ (3.0 kcal/mol)}$$

$$\text{and } \Delta S = 29 \text{ J K}^{-1} \text{ mol}^{-1}$$

The relative populations of the bonded conformer  $C_B$  were also obtained and listed in Table III. The present result for  $\Delta H$  is in good agreement with the earlier value (2.8 kcal/mol) obtained for a tetrachloroethylene solution by infrared spectroscopy.<sup>16</sup>

The above analyses also yields the following ratios:

$$I_N(n_N)/I_N(n_O) = 0.88 \text{ and } I_B(n_N)/I_B(n_O) = 0.62$$

It is noted that even in the nonbonded conformation  $I(n_N)$  is smaller than  $I(n_O)$ . This is apparently contrary to the observed ratio for  $\text{H}_2\text{NCH}_2\text{CH}_2\text{OH}$  ( $I(n_N) > I(n_O)$ ) in Figure 3. However, an explanation can be made in terms of effective solid angles open to incoming metastable atoms. In the dimethyl analogue, the

effective solid angle for the  $n_N$  orbital is decreased, as observed for some substituted anilines with methyl groups.<sup>7</sup> Such a steric effect may occur to a larger extent than one would expect for a small reagent like a proton, since the radius for  $\text{He}^*$  ( $2^3\text{S}$ ) is estimated to be as large as 2.5 Å. This estimate can be made from the van der Waals radius of Ne (1.5 Å) together with the fact that the  $\text{He}^*$  ( $2^3\text{S}$ )-Ne potential becomes repulsive even at a large distance of about 4.0 Å.<sup>17</sup>

**5. Concluding Remarks.** Formation of intramolecular hydrogen bonding was found to cause a considerable deactivation of the nonbonding orbitals in Penning ionization. Helium atoms in metastable states attack easily the nonbonding orbitals when (i) the molecule has no hydroxyl group accessible to the  $n$  orbitals or (ii) the molecule is in a nonbonded molecular conformation. For an intramolecular H-bonded conformer, however, the nonbonding orbital involved in the hydrogen bond is geometrically placed in the "shadow" of the OH bond and shows a considerably suppressed activity in electrophilic attacks by metastable helium atoms. When the dissociation equilibrium is shifted at higher temperatures and the steric shadow effect by the OH bond is decreased, the reactivity of the  $n$  orbitals increases, since much more electron density is then exposed to the exterior region accessible to the incoming species.

It is noted that Penning ionization is a typical process of electron-transfer reactions; an electron in an occupied molecular orbital of the sample molecule is extracted by an electrophile. The Penning process may thus be used to study relative reactivities of sample molecules. In this use, metastable rare gas atoms may be considered to be microscopic probes of the stereochemical properties of molecular orbitals in the sample molecule. The present study demonstrates that Penning ionization electron spectroscopy may find its applications not only to the comparative study of relative reactivities of orbitals for various molecules but also to the study of dynamic variations of reactivity due to conformational changes.

**Acknowledgment.** We thank T. Ishida and Y. Itoh for their help in calculations.

(16) Krueger, P. J.; Mettee, H. D. *Can. J. Chem.* 1965, 43, 2970-2977.

(17) Chen, C. H.; Haberland, H.; Lee, Y. T. *J. Chem. Phys.* 1974, 61, 3095-3103.

## Study of Stereochemical Properties of Molecular Orbitals by Penning Ionization Electron Spectroscopy. Effects of Through-Space/Through-Bond Interactions on Electron Distributions

Koichi Ohno,\* Toshimasa Ishida, Yukito Naitoh, and Yasuo Izumi

Contribution from the Department of Chemistry, College of Arts and Sciences, The University of Tokyo, Komaba, Meguro-ku, Tokyo 153, Japan. Received July 19, 1985

**Abstract:** Experimental evidence for effects of through-space/through-bond interactions on electron distributions of molecular orbitals was observed by Penning ionization electron spectroscopy. For norbornadiene, the next highest occupied molecular orbital, which has high electron densities in the endo face augmented by the through-space interactions between  $\pi$  electrons on the double bonds, showed a large reactivity upon electrophilic attacks by metastable helium atoms. In the case of 1,4-diazabicyclo[2.2.2]octane, the highest occupied MO composed of a symmetric coupling of the lone-pairs on nitrogen atoms, which has a smaller exterior electron density than the next HOMO because of the strong through-bond interactions, was found to give the smaller reactivity in Penning ionization.

Molecular orbitals have profound scientific meanings as they explain varieties of experimental results in systematic ways. Recent progress in the chemical orbital theory has made it possible to elucidate chemical reactions on the basis of MO calculations.

Even though such a relationship between theory and experiment is approximate, the relation cannot be limited to one way. One may, therefore, expect that an experimental study is able to elucidate a theoretical construct. A concrete example of this

possibility one should note here is the observation of molecular orbitals by utilizing a kind of reaction involving probe particles as well as sample molecules. One of the important reactions for this purpose is the (e, 2e) reaction;  $e^- + M \rightarrow M^+ + e^- + e^-$ . McCarthy, Weigold, and their collaborators have made extensive studies on (e, 2e) electron spectroscopy and have obtained valuable information on individual molecular orbitals.<sup>1,2</sup> Tossell et al. also reported such applications of the (e, 2e) technique.<sup>3-5</sup> In the (e, 2e) reaction, the incident electron plays the role of bringing the ionization energy as well as the role of the catalyst which cancels out in the apparent reaction of the molecule M,  $M \rightarrow M^+ + e^-$ . Another example is also an ionization reaction which involves rare gas atoms in metastable states, such as  $\text{He}^* (2^3\text{S}, 19.82 \text{ eV})$ ;  $\text{He}^* + M \rightarrow \text{He} + M^+ + e^-$ . This reaction is called Penning ionization, and the metastable atom plays the role of the electron receptor as well as the role of the ionization energy source in the electron-exchange mechanism;<sup>6</sup> an electron in an occupied orbital of the sample molecule is extracted into an inner-shell hole of the metastable atom, and an electron in the outer-shell orbital of the metastable atom is ejected into a continuum state with a kinetic energy nearly equal to the difference between the energy of the metastable state and the ionization energy. In our previous work, Penning ionization electron spectroscopy was applied to the study of electron distributions of molecular orbitals.<sup>7,8</sup> Some important features of Penning ionization are summarized as follows: (i) rare gas atoms in metastable states behave as electrophiles, (ii) rare gas atoms cannot penetrate through the repulsive surface of the target sample molecules, (iii) electron-transfer reactions are most likely to occur when the electrophile (the metastable atom) and the electron donor (the sample molecule) are in close contact to cause effective overlapping of both orbitals, (iv) orbitals exposed to the outside beyond the repulsive molecular surface react with electrophiles more easily than orbitals localized inside the molecular surface, and (v) a bulky group in the target molecule can act as a shield protecting a target orbital against attacks of electrophiles. On these findings, one may be encouraged to study stereochemical properties of molecular orbitals by the use of metastable atoms as a probe.

In spite of many successful applications of the molecular orbital theory, there are some problems for experimentalists in order to explain the results in terms of group orbitals or localized orbitals. In principle, usual SCF molecular orbitals (canonical molecular orbitals) can be obtained from a transformation of localized molecular orbitals<sup>9</sup> which are easily connected with chemical concepts, such as lone-pairs or functional groups. However, the transformation is purely mathematical and usually not deducible from some chemical insights. For example, the symmetry of a frontier orbital, which often plays an important role, is difficult to be seen from the localized or semilocalized scheme. Notable situations with such difficulties are encountered for molecules having a couple of equivalent lone-pairs or a couple of nonconjugated  $\pi$  bonds. An important contribution to this problem was made by Hoffmann, Imamura, and Hehre.<sup>10,11</sup> They introduced concepts of through-space/through-bond interactions which made it possible to bring a qualitative insight connecting the localized

or group orbital representation to the MO representation. Through-space/through-bond concepts have been successfully applied to analyses of IP values observed by photoelectron spectroscopy<sup>12-15</sup> as well as the study of spin-density distributions.<sup>16</sup>

The purpose of the present study is to observe the difference between symmetric and antisymmetric molecular orbitals caused by through-space/through-bond interactions of equivalent localized orbitals. The stress is placed on observation of the difference in spatial electron distributions of the molecular orbitals as well as their relative reactivities. The results obtained by Penning ionization electron spectroscopy demonstrate that the use of  $\text{He}^* (2^3\text{S})$  reactions has a potential value to observe stereochemical properties of molecular orbitals.

## Experimental Section

$\text{He}^* (2^3\text{S})$  Penning ionization electron spectra (PIES) and He I ultraviolet photoelectron spectra (UPS) were measured for norbornadiene and 1,4-diazabicyclo[2.2.2]octane (DABCO) by means of a transmission-corrected electron spectrometer.<sup>7,17</sup> The helium metastable atoms ( $2^3\text{S}, 19.82 \text{ eV}$ ) were produced with an electron gun and a quench lamp. The helium I resonance line (584 Å, 21.22 eV) was produced by a dc discharge. The electron energy spectra were obtained for electrons ejected at the angle of 90° with respect to the metastable helium beams or the photon beams by means of a hemispherical analyzer equipped with scanning electrodes at the entrance.

## Calculations

Molecular orbital calculations were performed at the computer center of the University of Tokyo. A library program GSCF2<sup>18</sup> was used for ab initio MO calculations. A split-valence type basis set (4-31G)<sup>19</sup> and the more extended basis set (HDD2G) were used for the basis functions. The HDD2G set includes the 6-311G functions<sup>20</sup> for hydrogen atoms and (1s7p)/[5s4p] functions for heavier atoms which were designed for calculations of Rydberg states by Dunning and Hay.<sup>21</sup> Exterior electron densities (EED) for occupied molecular orbitals were calculated with our program. The repulsive molecular surfaces were estimated from the conventional van der Waals radii of the atoms ( $r_{\text{C}} = 1.70 \text{ Å}$ ,  $r_{\text{H}} = 1.20 \text{ Å}$ ,  $r_{\text{N}} = 1.50 \text{ Å}$ ). Electron densities outside the molecular surface are counted for a cubic lattice with a lattice parameter  $d$ . The size of  $d$  was suitably chosen as indicated below. Exterior regions were divided into several parts with a thickness of 0.5 Å (from the inside region I, II, III, IV, etc.) to see the convergence character. Contributions from the regions farther than 2.0 Å from the molecular surface were found to be negligible for the HDD2G basis set even though it includes very diffuse primitive GTO's. For the 4-31G basis set, contributions due to the region IV (1.5–2.0 Å) were also found to be negligible. The lattice parameter  $d$  was chosen as follows in order to save computation time without losing accuracy;  $d = 0.05 \text{ Å}$  for the region I,  $d = 0.10 \text{ Å}$  for the region II,  $d = 0.30 \text{ Å}$  for the regions III and IV. Electron density contour plots were drawn for some molecular orbitals. The electron density of the  $n$ th line from the outside is  $k \times 2^n \times 10^{-4} \text{ au}^{-3}$ , where  $k$  is a parameter. In the electron density maps, thick solid curves

(1) McCarthy, I. E.; Weigold, E. *Endeavour*, **1978**, *2*, 72–79.

(2) Brion, C. E.; Hood, S. T.; Suzuki, I. H.; Weigold, E.; Williams, G. R. *J. J. Electron Spectrosc. Relat. Phenom.* **1980**, *21*, 81–87 and references cited therein.

(3) Moore, J. H.; Tossell, J. A.; Coplan, M. A. *Acc. Chem. Res.* **1982**, *15*, 192–198 and references cited therein.

(4) Tossell, J. A.; Moore, J. H.; Coplan, M. A.; Stefani, G.; Camilloni, R. *J. Am. Chem. Soc.* **1982**, *104*, 7416–7423.

(5) Hiser, S.; Chornay, D. J.; Coplan, M. A.; Moore, J. H.; Tossell, J. A. *J. Chem. Phys.* **1985**, *82*, 5571–5576.

(6) Hotop, H.; Niehaus, A. *Z. Phys.* **1969**, *228*, 68–88.

(7) Ohno, K.; Mutoh, H.; Harada, Y. *J. Am. Chem. Soc.* **1983**, *105*, 4555–4561.

(8) Ohno, K.; Matsumoto, S.; Harada, Y. *J. Chem. Phys.* **1984**, *81*, 4447–4454 and references cited therein.

(9) Edmiston, C.; Rüdenberg, K. *Rev. Mod. Phys.* **1963**, *35*, 457–465.

(10) Hoffmann, R.; Imamura, A.; Hehre, W. J. *J. Am. Chem. Soc.* **1968**, *90*, 1499–1509.

(11) Hoffmann, R. *Acc. Chem. Res.* **1971**, *4*, 1–9.

(12) Hoffmann, R.; Heilbronner, E.; Gleiter, R. *J. Am. Chem. Soc.* **1970**, *92*, 706–707.

(13) Broglie, F.; Heilbronner, E.; Ipaktschi, J. *Helv. Chim. Acta* **1972**, *55*, 2447–2451.

(14) Heilbronner, E.; Martin, H. D. *Helv. Chim. Acta* **1972**, *55*, 1490–1502.

(15) Heilbronner, E.; Muszkat, K. *J. Am. Chem. Soc.* **1970**, *92*, 3818–3821.

(16) Ohsaku, M.; Imamura, A.; Hirao, K.; Kawamura, T. *Tetrahedron* **1979**, *35*, 701–706.

(17) Harada, Y.; Ohno, K.; Mutoh, H. *J. Chem. Phys.* **1983**, *79*, 3251–3255.

(18) Kosugi, N. Program GSCF2, Program Library, The Computer Center, The University of Tokyo, Tokyo, Japan 1981.

(19) Ditchfield, R.; Hehre, W. J.; Pople, J. A. *J. Chem. Phys.* **1971**, *54*, 724–728.

(20) Krishnan, R.; Binkley, J. S.; Seeger, R.; Pople, J. A. *J. Chem. Phys.* **1980**, *72*, 650–654.

(21) Dunning, T. H., Jr.; Hay, P. J. "Methods in Electronic Structure Theory"; Schaefer, H. F., III, Ed.; Plenum: New York, 1977; pp 1–27.

**Table I.** Data for Norbornadiene

band	IP <sub>obsd</sub> /eV <sup>b</sup>	MO <sup>c</sup>	IP <sub>calcd</sub> /eV <sup>d</sup>		EED <sup>a</sup> (%)		I(PIES) <sup>e</sup>
			4-31G	HDD2G	4-31G	HDD2G	
1	8.71	6b <sub>2</sub>	8.484	8.725	2.943	4.705	1.000
2	9.56	10a <sub>1</sub>	9.499	9.729	3.842	5.772	1.334
3	11.34	6b <sub>1</sub>	12.417	12.629	1.571	1.733	
4	11.79	3a <sub>2</sub>	12.656	12.888	1.571	1.645	
5	12.14	5b <sub>2</sub>	13.124	13.343	2.009	2.061	
6	12.37	9a <sub>1</sub>	13.633	13.839	2.227	2.267	
7	12.70	8a <sub>1</sub>	14.251	14.484	2.142	2.211	
8	13.15	5b <sub>1</sub>	14.175	14.392	2.652	2.742	
9	14.18	4b <sub>2</sub>	15.267	15.486	2.307	2.260	
10	15.68	3b <sub>2</sub>	17.657	17.900	1.974	1.946	
11	16.44	4b <sub>1</sub>	18.333	18.529	1.945	1.903	
12	17.14	7a <sub>1</sub>	18.938	19.171	2.596	2.609	

<sup>a</sup>Exterior electron density. The EED is defined for each MO by the total electron density outside the repulsive molecular surface (see text).  
<sup>b</sup>Observed vertical IP from UPS. <sup>c</sup>Corresponding molecular orbital. <sup>d</sup>Theoretical IP from ab initio MO calculations with 4-31G and HDD2G basis sets. <sup>e</sup>Observed relative PIES band intensity.

indicate repulsive molecular surface. In order to compare relative PIES band intensities with calculated EED values, theoretical spectra were synthesized from Gaussian-type bands with area proportional to the respective EED values. Band positions and bandwidths were estimated from the observed spectra, since theoretical calculations of these quantities were not of interest in the present study. Although 4-31G calculations were found to be satisfactory for hydrocarbon molecules,<sup>8</sup> electron density contour plots and theoretical spectra in the present study were obtained from calculations with the HDD2G basis set which was found to be more reliable for molecules containing lone-pairs.<sup>22,23</sup>

## Results and Discussion

**1. Through-Space Interactions in Norbornadiene.** In Figure 1 He I UPS and He\* (2<sup>3</sup>S) PIES for norbornadiene are shown together with a theoretical spectrum for PIES synthesized from exterior electron densities (EED). Bands are labeled by numbers from the left and assigned to relevant molecular orbitals from which electrons are ejected upon ionization. Table I lists vertical IP values obtained from the UPS and calculated IP values obtained from MO calculations via Koopmans' approximation. Band 1 is assigned to the 6b<sub>2</sub> orbital (π<sub>a</sub>) made of an antisymmetric coupling of π electrons on two separated double bonds. Band 2 is assigned to the 10a<sub>1</sub> orbital (π<sub>s</sub>) composed of a symmetric coupling of π electrons. The through-space interaction involving in-phase coupling of the p orbitals in the endo face causes a considerable stabilization of the symmetric MO (π<sub>s</sub>). Heilbronner et al.<sup>10-13</sup> discussed the relative order of the two types of π orbitals for norbornadiene and its analogues. They concluded from comparative studies of observed IP values that for norbornadiene the highest occupied MO(HOMO) is of antisymmetric type. The present study of PIES gives a confirmation of this ordering from different aspects of these molecular orbitals.

It is of note that in the PIES band 2 corresponding to the next HOMO (π<sub>s</sub>) is enhanced with respect to band 1 which is due to ionization from the HOMO (π<sub>s</sub>); the integrated band area is much larger for band 2 in PIES (Table I). This indicates that ionization caused by electrophilic attacks of metastable helium atoms is more likely to occur at the symmetric π orbital (10a<sub>1</sub>) rather than the antisymmetric one (6b<sub>2</sub>). The relative reactivities for these orbitals are qualitatively understood from the electron density contour plots shown in Figure 2; exterior electron distributions outside the repulsive molecular surface for the symmetric orbital (π<sub>s</sub>, 10a<sub>1</sub>) are much larger than those for the antisymmetric orbital (π<sub>a</sub>, 6b<sub>2</sub>). Since metastable helium atoms attack exterior electrons outside the molecular surface, electrons are much more likely to be extracted from the symmetric orbital. This nature of the reactive electron distributions in the endo face for the next HOMO (π<sub>s</sub>, 10a<sub>1</sub>) may be connected with a formation of metal carbonyl compounds, such as norbornadiene-Fe(CO)<sub>3</sub>.<sup>24</sup>

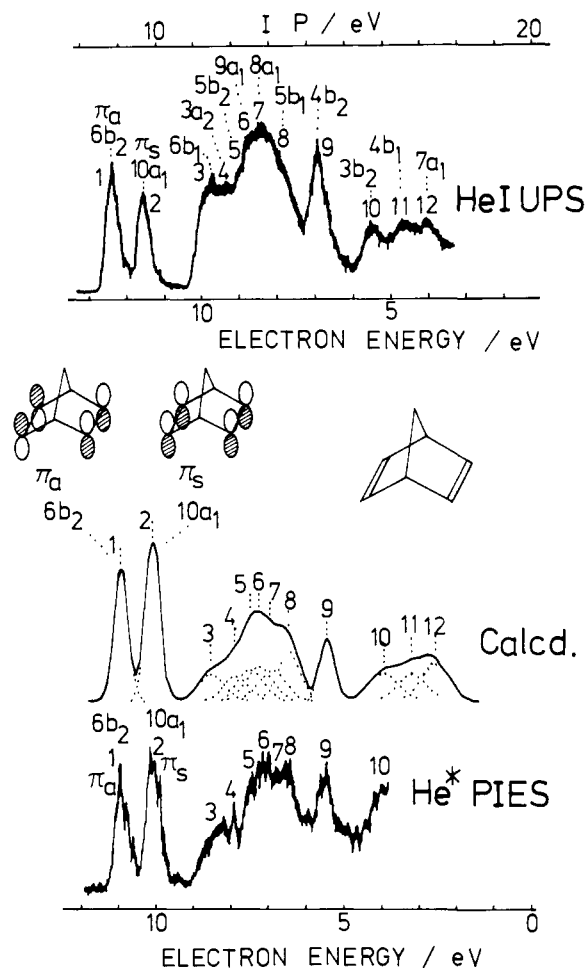


**Figure 1.** He\* (2<sup>3</sup>S) Penning ionization electron spectrum (PIES, bottom), theoretical Penning spectrum calculated from EED (calcd, middle), and He I photoelectron spectrum (UPS, top) for norbornadiene.

The more quantitative analyses can be made for the PIES on the exterior electron model;<sup>7,8</sup> the integrated band area or the Penning ionization probability has been supposed to be proportional to the exterior electron density (EED) integrated over the region outside the molecular surface. Table I includes EED values obtained for two types of basis sets. The EED values are shown in the unit of 10<sup>-2</sup> or percent (%). In Figure 1, a synthesized spectrum from the EED values (HDD2G) gave good agreement with the observed PIES. This provides a confirmation of the

(22) Ohno, K.; Matsumoto, S.; Harada, Y. *J. Chem. Phys.* **1984**, *81*, 2183-2184.

(23) Ohno, K.; Ishida, T. *Int. J. Quantum Chem.*, to be published.

(24) King, R. B. "Organic Chemistry of Iron"; Koerner von Gustorf, E. A., Grevels, F.-W., Fishler, I. Eds.; Academic Press: New York, 1978; Vol. 7, pp 525-625.

Table II. Data for 1,4-Diazabicyclo[2.2.2]octane

band	IP <sub>obsd</sub> /eV <sup>b</sup>	MO <sup>c</sup>	IP <sub>calcd</sub> /eV <sup>d</sup>		EED <sup>a</sup> (%)		I(PIES) <sup>e</sup>
			4-31G	HDD2G	4-31G	HDD2G	
1	7.60	6a <sub>1</sub> '	8.225	8.343	2.892	3.546	1.000
2	9.64	5a <sub>2</sub> ''	11.335	11.378	3.259	4.250	1.754
3	11.10	4e''	12.303	12.425	2.363	2.396	
4	11.53	1a <sub>1</sub> ''	12.853	12.941	1.710	1.730	
5	12.66	5e'	14.112	14.243	1.904	1.823	
6	13.29	4e'	14.785	14.902	2.494	2.460	
7	13.88	3e''	15.492	15.600	1.792	1.792	
8	14.37	1a <sub>2</sub> '	15.760	15.842	2.022	2.039	
9	15.90	5a <sub>1</sub> '	18.107	18.188	2.515	2.483	
10	16.33	3e'	18.586	18.694	2.017	1.996	
11	17.10	4a <sub>2</sub> ''	19.389	19.455	1.868	1.927	

<sup>a</sup> Exterior electron density. As for degenerate orbitals (e' or e'') the EED value for a single moiety is listed. <sup>b</sup> Observed vertical IP from UPS. <sup>c</sup> Corresponding molecular orbital. <sup>d</sup> Theoretical IP from ab initio MO calculations with 4-31G and HDD2G basis sets. <sup>e</sup> Observed relative PIES band intensity.

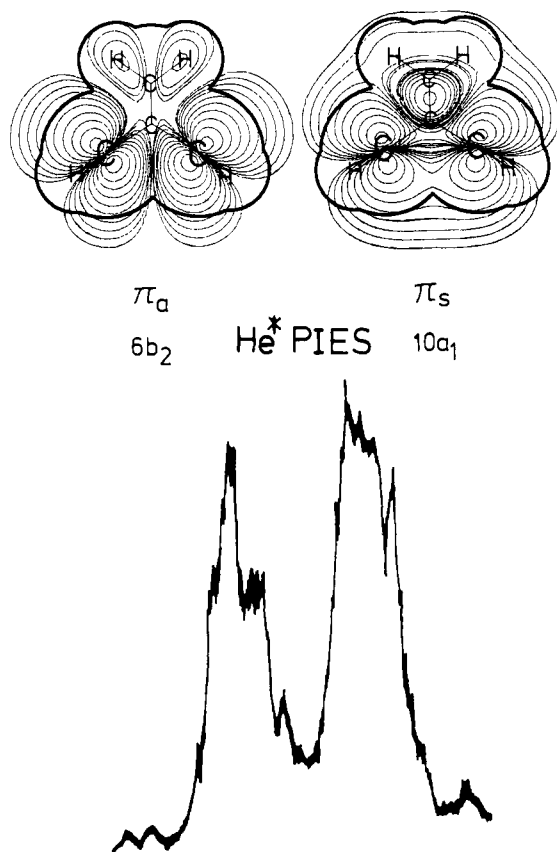


Figure 2. He\* PIES and electron density contour plots of the antisymmetric  $\pi$  orbital ( $\pi_a$ ,  $6b_2$ ) and the symmetric  $\pi$  orbital ( $\pi_s$ ,  $10a_1$ ) for norbornadiene. The contour plots were drawn for a plane perpendicular to the double bonds and included two carbon atoms on the double bonds. The electron density of the  $n$ th line from the outside is  $0.5 \times 2^n \times 10^{-4} \text{ au}^{-3}$ . Thick solid curves in the maps indicate the repulsive molecular surface.

conclusions given above from qualitative discussions. The EED calculations also suggest that the level ordering of the  $8a_1$  and the  $5b_1$  orbitals may be reversed as indicated in Table I.

In addition, one must note again that the through-space interactions occur at the endo face where p orbitals for  $\pi$  electrons on two separated double bonds overlap effectively. A different situation is found for 1,4-cyclohexadiene. It also involves a cyclic-diene structure, but the geometry is nearly flat so that it is difficult for the p orbitals on separated double bonds to overlap effectively. This is consistent with an observation in the previous study;<sup>8</sup> EED values as well as PIES band intensities were found to be nearly the same for symmetric and antisymmetric  $\pi$  MO's in 1,4-cyclohexadiene.

**2. Through-Bond Interactions in 1,4-Diazabicyclo[2.2.2]octane (DABCO).** In Figure 3 He I UPS, He\* ( $2^3S$ ) PIES, and a

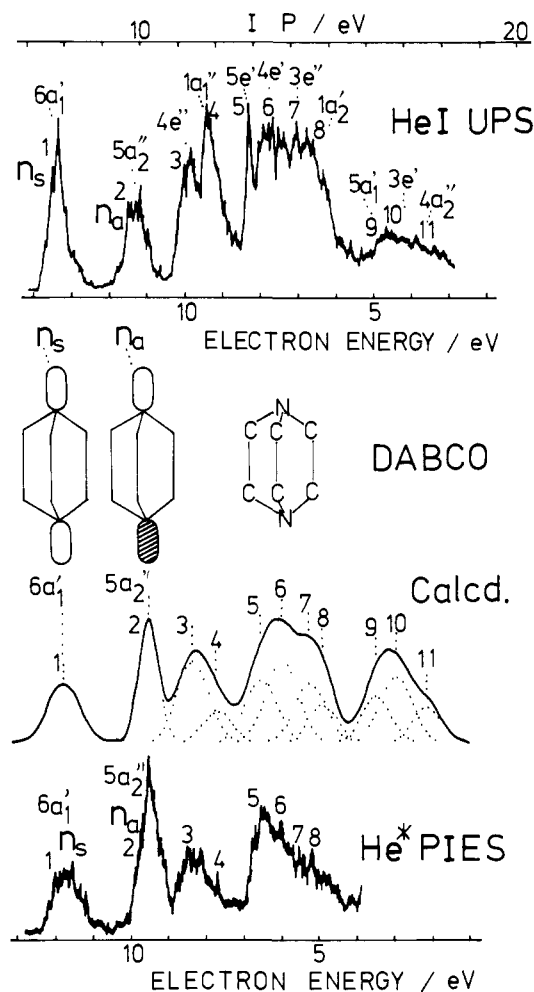
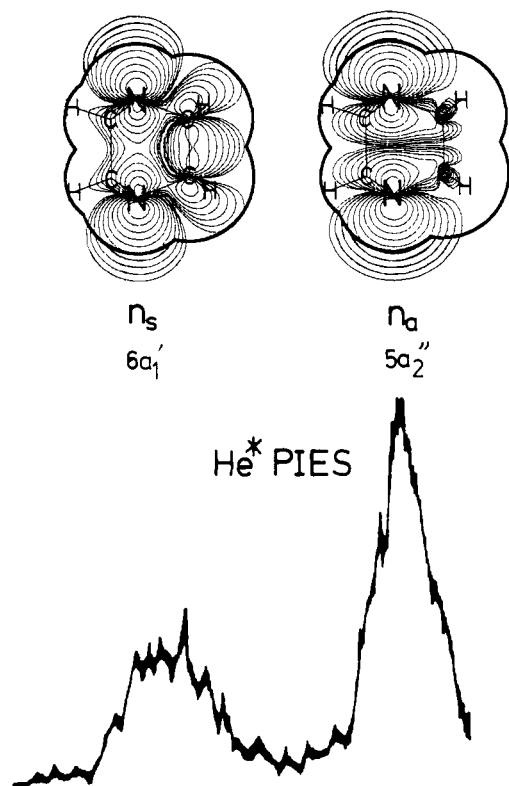


Figure 3. He\* ( $2^3S$ ) Penning ionization electron spectrum (PIES, bottom), theoretical Penning spectrum calculated from EED (calcd, middle), and He I photoelectron spectrum (UPS, top) for 1,4-diazabicyclo[2.2.2]octane.

theoretical spectrum from EED/HDD2G are shown from DABCO. The observed bands are assigned to molecular orbitals. Table II lists the observed vertical IP, calculated IP, EED, and observed band area for PIES. The bands 1 and 2 are assigned to symmetric and antisymmetric couplings of nitrogen lone-pair electrons, respectively; the HOMO is a symmetric nonbonding MO ( $n_s$ ,  $6a_1'$ ) and the next HOMO is an antisymmetric one ( $n_a$ ,  $5a_2''$ ).<sup>15</sup> Assignments of other bands can also be made on the basis of calculated IP values (Table II).

In the PIES, an emphasis must be placed on the remarkable enhancement of band 2 with respect to band 1. This indicates that the next HOMO ( $n_a$ ) composed of an antisymmetric coupling



**Figure 4.** He\* PIES and electron density contour plots of the symmetric nonbonding orbital ( $n_s$ ,  $6a_1'$ ) and the antisymmetric nonbonding orbital ( $n_a$ ,  $5a_2''$ ) for 1,4-diazabicyclo[2.2.2]octane. The contour plots were drawn for a plane including a couple of nitrogen atoms as well as a C-C single bond. The electron density of the  $n$ th line from the outside is  $0.25 \times 2^n \times 10^{-4} \text{ au}^{-3}$ . Thick solid curves in the maps indicate the repulsive molecular surface.

of nitrogen lone-pair is much more reactive than the HOMO ( $n_s$ ) of symmetric type. This observation is qualitatively understood from Figure 4 where electron densities for the  $n_a$  orbital are much more exposed to the exterior region than those for the  $n_s$  orbital. It is also seen in Figure 4 that through-bond interactions involving the C-C bonds for the  $n_s$  orbital result in a considerable reduction of exterior electron distributions on the nitrogen atoms. On the other hand for the  $n_a$  orbital, such a through-bond interaction is forbidden from its symmetry requirement with a nodal plane bisecting the C-C bonds. The theoretical spectrum obtained from the EED values (Figure 3) also demonstrates that the  $n_a$  orbital is more reactive than the  $n_s$  orbital in Penning reaction. It is in addition noted that band 4, which is clearly seen in the UPS, is almost missing in the PIES. This is explained from the small EED

value for the corresponding orbital ( $1a_1''$ ) (Table II).

**3. Concluding Remarks.** Effects of through-space/through-bond interactions on electron distributions of molecular orbitals were observed by the use of metastable helium atoms. In norbornadiene, a symmetric and constructive coupling between geometrically separated  $\pi$  electrons on two double bonds causes an augmentation of electron densities in the endo face. This effect of the through-space interactions results in the higher reactivity of the symmetric  $\pi$  orbital ( $\pi_s$ ,  $10a_1$ ) upon electrophilic attacks by metastable helium atoms. In DABCO, a symmetric coupling between a couple of lone-pairs having most of their electron densities toward opposite directions involves bonding interactions through the C-C bonds and yields a symmetric nitrogen-nonbonding orbital ( $n_s$ ,  $6a_1'$ ) with relatively small electron densities on the nitrogen atoms. This leads to the observation that the next HOMO ( $n_a$ ,  $5a_2''$ ) of antisymmetric type without the through-bond effect shows a larger reactivity than the HOMO ( $n_s$ ,  $6a_1'$ ) of symmetric type.

It is worthy to note that the orbital symmetry is not necessarily coherent with the orbital activity in Penning reaction; in norbornadiene  $\pi_s > \pi_a$ , while in DABCO  $n_a > n_s$ . One may deduce the following principles from the present results. (1) When a through-space interaction causes a constructive superposition of localized orbitals, it pumps up inner-electron densities to result in an enhancement of exterior-electron densities for the symmetric MO. This is highly likely because the spatial region, where the through-space interaction is most effective, is usually the reactive region outside the repulsive molecular surface. (2) When a through-bond interaction introduces a strong bonding character between certain bonded atoms, an absorption of exterior-electron densities into the inner inactive region occurs for the symmetric MO. This is quite natural since the through-bond interaction is only operative inside the repulsive molecular surface.

These findings carry two important messages: (i) the concept of through-space/through-bond interactions<sup>10,11</sup> is of great importance to discuss spatial distributions of molecular orbitals, especially for systems having lone-pairs, nonconjugated  $\pi$  electrons, or some functional groups and (ii) change in electron distributions as well as reactivity can be probed for individual occupied molecular orbitals experimentally by the use of He\* ( $2^3S$ ) reactions.

Finally one may comment on the basis-set dependence of the calculations. In a qualitative understanding, a middle size basis set (4-31G) was found to be satisfactory. From a quantitative point of view, theoretical spectra synthesized from the EED values gave much better agreement with experiment when the more extended basis set was used. This indicates that the PIES technique combined with the EED model may be used to study the quality of wave function tails which depend sensitively on the choice of basis functions in the *ab initio* MO calculations.

**Acknowledgment.** We thank Professor Y. Harada for helpful comments and Dr. S. Masuda for his help in the experiments.